Title
Anomalous current ratios in phosphoric acid fuel cell cathodes

Author
Ross, P.N.

Publication Date
1986-03-01

Lawrence Berkeley Laboratory
UNIVERSITY OF CALIFORNIA

Materials & Molecular Research Division

Submitted to Journal of the
Electrochemical Society

ANOMALOUS CURRENT RATIOS IN
PHOSPHORIC ACID FUEL CELL CATHODES

P.N. Ross, Jr.

March 1986

Prepared for the U.S. Department of Energy under Contract DE-AC03-76SF00098

DISCLAIMER

ANOMALOUS CURRENT RATIOS IN PHOSPHORIC ACID FUEL CELL CATHODES

Philip N. Ross, Jr.

Lawrence Berkeley Laboratory
Materials and Molecular Research Division
University of California
Berkeley, CA 94720

INTRODUCTION

One of the most significant advances in phosphoric acid fuel cell technology in recent years has been the development of pressurized systems.[1] Pressurization increases the power density of the fuel cell stack without sacrificing any overall thermal efficiency if the turbo-compressor can be run off the waste heat in the system.[2] In current electric utility power plant applications,[3] the process air is turbo-charged to 470 kPa (absolute) which enables the cell stack to operate at twice the current density (400 mA/cm^2) of an ambient pressure stack at the same overall thermal efficiency. There is, therefore, considerable interest in the nature of the voltage losses in gas diffusion electrodes occurring at much higher current densities than normal. As we show in this work, one does not observe a first order dependence of current density at constant cathode potential in phosphoric acid fuel cell electrodes in the region of current density of practical interest (200-400 mA/cm^2). The kinetics of oxygen reduction on smooth Pt in concentrated phosphoric acid is first-order in oxygen partial pressure,[4] i.e. the current at fixed electrode potential (not overpotential) increase linearly with oxygen partial pressure. It is

easily shown [5] that polarization due to slow oxygen transport either by liquid phase diffusion of dissolved oxygen or by gas-phase diffusion of molecular oxygen [6] does not change the apparent reaction order when the kinetics are first order. It seems appropriate, therefore, to refer to the non-linearincreases in current density with oxygen pressure as anomalous current ratios, as they are unexpected from either the reaction kinetics or from the diffusion processes usually considered dominant in fuel cell electrodes.[7]

The fuel cell cathodes used in this work were prepared in this laboratory using several different procedures, and the polarization curves observed with these electrodes were comparable to those reported for commercial fuel cell electrodes. The observation of anomalous current ratios was not restricted to either a particular type of electrode structure or to a particular Pt electrocatalyst, but rather it was observed with almost any type of gas diffusion electrode made with a Pt catalyst. However, for practical purposes, the results presented here are for electrodes that, to the best of our knowledge, represent the type of air cathode currently used in phosphoric acid fuel cell systems.

EXPERIMENTAL

Two types of Pt on carbon black catalyst were used. One was a commercially available (Prototech) fuel cell catalyst containing 10 w/o Pt dispersed on a Vulcan XC-72R carbon black. This catalyst was prepared via a colloidal method described in the patent literature,[8] and requires either heat treatment at ca. 673 K or hydrogen reduction at ca. 423 K to reduce the adsorbed colloidal particles to metallic (zero valent) Pt. Here we used hydrogen reduction at 423 K as the standard reducing pretreatment. The nominal Pt surface area measured via the carbon monoxide adsorption method[9] was 120 m^2g. The other catalyst was prepared using a graphitized carbon support produced by heat treating Vulcan XC-72R at 3000 K in a helium atmosphere (noted as GV in subsequent text). This support was catalyzed via an ion-exchange method. Acid sites were introduced onto the carbon surface by oxidation with chromic acid (2 hrs., 373 K). The complex cation $Pt(NH_3)_4^{2+}$ was ion-exchange controlled by adjusting solution pH. The highly alkaline base $Pt(NH_3)_4(OH)_2$ was prepared by passing a platinum tetramine chloride solution through an anion exchange resin (Amberlite IRA-400, Rohn and Haas) to convert the chloride to hydroxide. The basic platinum solution was added dropwise to a water slurry of the oxidized carbon with continuous monitoring of the pH until the pH reached ca. 12. After filtration, water washing, and air drying, the catalyst was reduced in hydrogen at 423 K for two hours. The Pt loading was $5 \pm .05$ wt. % and the nominal Pt surface area measured via the carbon monoxide adsorption method was 88 m^2g.

The type of gas diffusion electrode used here was the same as that used in commercial fuel cells. Basically it consists of a catalyst layer containing a hydrophobic gas pore forming agent (Dupont TFE 30B) distributed on a porous carbon paper substrate (Stackpole PC 206). The carbon paper substrate was wetproofed by impregnation with fluorinated ethylene propylene solids (Dupont FEP 120) to 25 w/o and air curing at 623 K for 900 sec. The carbon paper substrate acts as a gas permeable current collector that prevents a liquid film from forming between the gas stream and the catalyst layer. The in-plane conductivity of the carbon paper is ca. 0.02 Ω-cm, so the potential drop even at 1 A/cm^2 is less than 5 mV across the back of a small (e.g. 1 cm^2) electrode in a half-cell where current is taken off the edge. In a more practical size (>100 cm^2), the potential drop would be significant if current were taken off at the edge, but in practice, these electrodes are used in a bipolar stack with the current path normal to the plane of the paper. There are a number of ways in which the catalyst layer can be applied to the substrate and the fuel cell patent literature implies that the best performing electrodes can only be attained via the practice of wondrous art. In the course of this work, many different methods were examined, including some of the wondrous art called for in patents. In our experience, the end result does <u>not</u> vary greatly with method provided one uses a sufficiently low loading of catalyst (<2.5 mg/cm^2). A fabrication method was developed which was simple, easily translated to other laboratories with reproducible results, yet produced polarization behavior characteristic of commercial cathodes. The method was vacuum filtration of an aqueous suspension of catalyst and TFE 30B directly through the carbon

paper. The suspension was 1:1 isopropanol : water containing 20 g/ℓ catalyst and 7-20 g/ℓ TFE solids. The filtration substrate was coarse fritted glass, and during filtration the suspension was maintained via ultrasonic agitation. The as- filtered catalyst layer was air-dried several hours at 393 K, then hand-rolled to eliminate "mud-cracking." The electrode then received a final air curing at 613 K for 900 sec. It should be noted that this final curing temperature is above the melting point of TFE 30 B.

The polarization curves for the oxygen cathodes were measured in a three-electrode cell of unconventional design. Because of the relatively high current densities (up to 1 A/cm^2) used and the importance of current distribution and Ohmic losses at high current density, a new cell was designed that has the same current distribution as in a fuel cell and a method was developed for very accurate correction of the Ohmic drop in the electrolyte external to the cathode. An assembly diagram of the cell is shown in Fig. 1. It is essentially a free-electrolyte H_2-O_2 fuel cell, constructed entirely of Teflon, having a circular 1 cm^2 active area that is fitted with a reference electrode. The working electrode was an oxygen cathode fabricated as described above; the counter electrode was a gas-fed hydrogen electrode of a fuel cell type purchased from Prototech (Type RA-2); the reference electrode was a conventional hydrogen electrode fabricated from Pt black on a Pt mesh. The reference capillary aperature is flush with the side wall of the interelectrode gap so as not to intercept the current path between the current generating electrodes. Due to possible anomalies in the current flow along the side-wall, the conventional current-interruption method of IR-compensation for the potential drop in

solution between the reference capillary aperature and the cathode surface was supplemented by another method. The absolute resistance of the electrolyte in the gap was measured in-situ using standard AC impedance methods, and the cell potential was corrected at each current density by calculation of the IR-drop. The polarization of the counter electrode was measured independently by operating the cell with hydrogen at both electrodes, and this small correction (less than 5 mV at 500 mA/cm^2) applied to the IR-corrected cell potential to obtain the IR-free cathode potential (versus a reversible hydrogen electrode in the same electrolyte, RHE). The two different methods yielded nearly identical ($\pm$2 mV) IR-free potentials even in the highest current density region. The curves reported here are those obtained using the current-interruption method. Current-potential curves were recorded with a PAR 173 Potentiostat in the galvanostatic mode for highest accuracy in IR-correction.

The electrolyte was Mallinckrodt orthophosphonic acid purified by the method of Ferrier, et al.[11] and concentrated by evaporation of the excess water at 573 K as required. Both oxidant and hydrogen gases were presaturated with water vapor so that ll gases in the cell contained water in equilibrium with the bulk electrolyte according to the vapor pressure data of McDonald and Boyack.[12] The oxidant gases were calibrated mixtures (Matheson Ultra-High Purity Grade). The hydrogen was Matheson Extra-Dry Grade. All gases were used without further purification.

RESULTS

The characteristic variation in current-potential behavior of these supported Pt electrodes with oxygen partial pressure is shown in Fig. 2 for concentrated H_3PO_4. At this temperature and acid concentration the resistivity of the electrolyte was 1.6 Ω-cm. Below 50 mA/cm^2, the current ratios were 5:1, as expected from the kinetics of oxygen reduction. Above 50 mA/cm^2, the current ratio drops significantly below 5:1, with the ratio apparently approaching a minimum value of about 2.8 as shown in Fig. 3. This minimum ratio was observed to be independent of the thickness of the catalyst layer, but differed between two types of catalysts used. Figure 4 shows the current ratios observed with the Vulcan support catalyst layer which were qualitatively similar to the graphitized Vulcan support layer in Fig. 3 but with the current ratio reaching a minimum value of about 3.5. The differences in the minimum current ratios appears to be related to catalyst layer thickness. The catalyst layers each contained 0.25 mg Pt/cm^2, and the catalyst layer thicknesses were 0.004 ($\pm$ 10%) cm for 10 wt. % Pt on Vulcan and 0.008 ($\pm$ 10%) cm for 5 wt. % Pt on GV as determined by optical microscopy of electrode cross-sections. For each catalyst, variation in catalyst layer thickness changed the current density at which current ratios deviated from first order; a more detailed description of the effect of catalyst layer thickness is given later in this section. Phosphoric acid concentration was not found to have a significant effect on the slope of current-potential curves or on the magnitude of the current

ratios within the range of concentration (85-100 wt. %) and temperature (373-450 K) one might expect to use in fuel cells. However, in this range of concentration and temperature the conductivity of H_3PO_4 does not change profoundly, e.g. from a maximum of 0.6 mhos to a minimum of 0.4 mhos.

The association of the anomalous current ratio with electrolyte conductivity is suggested by two features in the current-potential curves. First, the current density at which the logarithmic plots deviate from linearity is at the same current density for all three partial pressures. The second feature is that the deviation of the observed potential from that expected if the current ratio were 5:1 is linearly related to current density. This is shown by a graphical construction method in Figure 6. The dotted curves show the expected log I - E relation if the current ratio were actually 5:1 obtained by multiplying the 20% O_2 curve by 5. If we call this deviation $\Delta\Phi_R$, the plot of against the current density is reasonably linear as seen from Fig. 6. It is convenient to refer to this $\Delta\Phi_R$ as "resistance polarization" and to determine the "internal resistance" from the slopes in Fig. 6, e.g. the slope was 10 mV per 100 mA/cm^2 when the thickness of the catalyst layer was 0.008 cm, so the apparent internal resistivity of the electrolyte filled pores was 12 Ω-cm. This value is about 6 times the resistivity of the bulk electrolyte. Note that the slopes of these plots varied directly with layer thickness, i.e. doubling the layer thickness doubled the slope.

Anomalous current ratios are not unique to gas-diffusion electrodes fabricated in our laboratory. The polarization curves we report here are typical of those reported for commercial fuel cell electrodes using similar

catalysts. Figure 7 shows the oxygen and air polarization curves for a commercial fuel cell cathode (from Energy Research Corporation, Danbury, CT) with 5 mg/cm^2 of 10 w/o Pt on Vulcan XC-72R at essentially the same conditions as Fig. 5. Note that the commercial electrode had a O_2:air current ratio of about 3.5 at high current density and 4.8 (the theoretical ratio for O_2:air) at low current density.

DISCUSSION

The polarization curves in which the anomalous current ratios were observed were corrected for the ohmic potential difference between the reference electrode capillary and the cathode by the current interruption technique. In the case of a porous electrode, the very fast ($<10^{-6}$ sec) drop in the potential transient corresponds to the potential difference between the reference capillary tip and the potential at the pore mouth, i.e. the geometric exterior of the electrode surface.[13] The potential drop in liquid filled pores within the catalyst layer decays with a much slower time constant ($>10^{-3}$ sec) as described in detail by Urbach.[14] When the external current path is broken, an internal current continues to flow through the pore until the internal polarization gradients have completely decayed, so that the resistive loss inside the pore becomes a component of the polarization decay with characteristic time constant $>10^{-3}$ sec.

This is certainly not the first time electrolyte conductivity has been shown to have an effect on the polarization behavior of fuel cell electrodes. In addition to the very early work of Urbach, more recent

porous electrode models by Iliev[15] and Iczkowski and Cutlip[16] have included a term for the variation in potential down an electrolyte filled pore. In fact, Iczkowski and Cutlip applied their model to the same type of cathode at the same conditions of temperature and acid concentration as that used here. The intent of their analysis was to make a determination of the sources and relative extents of the voltage loses in fuel cell cathodes. The result was somewhat surprising in view of the prior emphasis in the fuel cell literature on losses due to limiting liquid-phase transport of dissolved oxygen in "flooded agglomerates."[17] The analysis by Iczkowski and Cutlip indicated the major voltage loss in the fuel cell cathode at 200 mA/cm^2 on air was what they termed "ohmic resistance" in the catalyst layer, e.g. 13.3 mV or 6.7 mV per 100 mA/cm^2. In this work we have shown that via a model independent analysis of current ratios an apparent internal ohmic resistance can be determined which is 10-20 mV at 200 mA/cm^2. But this resistance effect was linear with current density only over a limited range of current density, and according to Fig. 3 $\Delta\Phi_R$ approaches a limiting value. This phenomenon was not described previously. Iliev[15] and Iczkowski and Cutlip[16] treated ionic conduction in liquid filled pores via Ohm's Law. As the author had pointed out previously,[17] this treatment is not fundamentally correct in a concentrated acid electrolyte. A purely ohmic potential drop occurs only when there is excess supporting electrolyte, which is not the case here. The physical situation in a fuel cell cathode is shown in Fig. 8 depicting a single liquid filled pore. The catalyst layer consists of interconnected porous catalyst particles saturated with electrolyte interspersed with hydrophobic Teflon solids which form the gas

pores. Hydrogen ion is consumed at the catalyst surface according to the overall stoichiometry of the reaction,

$$O_2 + 4\ (HS^+) + 4e^- \rightleftharpoons 2\ H_2O$$

where HS^+ represents the solvated state of the proton in this very concentrated medium. At sufficiently high rates of HS^+ consumption (current density) ionic conduction down the liquid pore cannot maintain invariant HS^+ concentration, and a liquid diffusion potential forms. The result is a resistance polarization[18] consisting of a purely ohmic potential drop and of a liquid diffusion potential as a result of the concentration gradient. As pointed out by Vetter[18] these two components of polarization have different characteristic time constants, the ohmic component a very small time constant, and the liquid junction potential has the time constant of a diffusion process. The so- called IR-correction that one makes using current interruption with fuel cell cathodes is the ohmic part of the resistive drop in the bulk electrolyte between the solid surface of the electrode and the reference capillary. There will, in general, be a liquid junction potential in the diffusion layer on the exterior surface of the electrode as well as the total (ohmic plus diffusion) resistance polarization within the catalyst layer. The liquid junction potential exterior to the electrode can, however, be minimized by bringing the reference electrode sufficiently close to the electrode surface.

In a strong acid electrolyte, one might not expect a significant liquid diffusion potential because of the very high concentration of proton

species. However, phosphoric acid is a relatively weak acid (pK_1 = 2.12 versus -3 for sulfuric acid) that is incompletely dissociated, and requires fast equilibrium between H_2O, H_3PO_4 and H_3O^+ to buffer the electrolyte, i.e. as hydrogen ion is depleted by reaction with oxygen, undissociated H_3PO_4 dissociates to provide more hydrogen ion. Slow transport of neutral H_3PO_4 will, therefore, cause a liquid diffusion potential to occur at sufficiently high rates of H_3O^+ depletion. The hydrogen ion concentration in the very concentrated electrolytes used here is not known, nor easily measured. There is indirect evidence that the hydrogen ion concentration drops significantly in going from 85 w/o acid to 100 w/o acid, in that the oxygen reduction kinetics, which are proportional to hydrogen ion concentration,[19] are dramatically reduced in the more concentrated medium. A rigorous treatment of the ionic transport processes is, however, further complicated by the existance of other possible ionic species in solution, due both to the autoprotolysis of H_3PO_4,

$$2\ H_3PO_4 \rightleftharpoons H_4PO_4^+ + H_3PO_4^-$$

and polymerization of the acid to form polyanions. A detailed and precise description of the transport processes in the liquid phase would have to include the neutral molecules O_2, H_2O and H_3PO_4, the solvated protons (e.g. $H_9O_4^+$, $H_4PO_4^+$), the anions and polyanions and would require knowledge of all the equilibrium relations between individual species and the individual ionic mobilities. Few of the required constants are known, so rigorously correct transport equations would not only be very complex, but contain a

large number of indeterminant parameters.

There appears to be some merit to an approximate description of the ionic conduction processes that is certainly more correct than assuming only ohmic resistance, but is not a complete description of all ionic species. The approximate description proposed here is a lumped parameter model, in which the electrolyte is treated as a binary electrolyte with an effective valence Z and effective ionic diffusion coefficient D_e. As shown by Vetter,[18] the sum of the purely ohmic potential drop and the liquid junction potential (resistance polarization) has the mathematical form of a diffusion potential with lumped parameters. Therefore, the resistance polarization can be treated mathematically using Fick's law with constants which may not have physical significance. A similar mathematical treatment of ionic conduction in hydrophobic gas-diffusion electrodes was used by Vdovichenko[20] with an approximate analytical solution obtained by perturbation theory. A mathematical treatment of resistance polarization that follows Vdovichenko's method is given in the Appendix for the case of air cathodes. Four different limiting cases were derived representing different regions of polarization with increasing current density:

i.) kinetic polarization

$$I = K_1 \delta R \gamma k C_o \exp(-2.3V/b)$$

ii.) kinetic + resistance polarization

$$I = (K_2 R \gamma k C_o)^{1/2} \exp(-2.3V/2b)$$

iii.) kinetic + oxygen diffusion polarization

$$I = 2K_1 \delta (nFD_m \gamma k)^{1/2} C_o \exp(-2.3V/2b)$$

iv.) kinetic + oxygen diffusion + resistance polarization

$$I = 2K_2^{1/2} (nFD_m\gamma k)^{1/4} C_o^{1/2} \exp(-2.3\ V/4b).$$

At low current densities, sufficiently small agglomerate sizes and sufficiently conducting electrolytes, the polarization is purely kinetic, with the slope of the log I - V curve being the kinetic Tafel slope b (about 100 mV for concentrated phosphoric acid). At higher current density, the apparent slope of the log I - V curve changes from b to 2b, due either to resistance polarization or to oxygen diffusion polarization. Which transport process becomes limiting depends on the relative rates and characteristic distances for HS^+ conduction and dissolved oxygen diffusion. When resistance polarization is the predominant transport limiting process, the current density is no longer first order in oxygen pressure, but rather depends on oxygen pressure to one-half power, e.g. the the current ratios here should be 2.24. At even higher current densities, the slope of the log I - V curve should show another transition from 2b to 4b, and in the regions of the limiting current the current ratios should be proportional to oxygen pressures to the half power. Thus, the model proposed correctly predicts, at least qualitatively, the occurrence of anomalous current ratios of approximately the right value (2.24 vs. 2.8) at sufficiently high current densities. It also predicts the observed transition to another linear log I - V region, although the observed slope (ca. 160 mV per decade) is not twice the kinetic slope (ca. 100 mV per decade) as expected. However, the model does not predict a minimum in the current ratio, as observed.

The mathematical representation of resistance polarization as a diffusion process in a binary electrolyte implies the existance of an ionic conduction limiting current due to complete exhaustion of hydrogen ion in the electrolyte-filled catalyst pores. This is physically incorrect, and in the particular case of H_3PO_4 the autoprotolysis equilibrium provides additional buffering capacity not accounted for in the model. Therefore, in the limiting current region oxygen transport processes are dominant, a conclusion that was also made by Iczkowski and Cutlip. As suggested in their work, the measurement of the limiting currents in O_2/He mixtures versus O_2/N_2 mixtures enables one to distinguish gas diffusion from liquid phase diffusion as the dominant oxygen transport resistance. These measurements indicated gas phase diffusion is the current limiting process in fuel cell electrodes of this type.

Although there are, clearly, fundamental inadequacies in the treatment of the ionic conduction phenomena presented here, there seems to be little or no practical merit in deriving more rigorous models of ionic conduction that require numerical solution of the equations. The analytic equations derived here embody the correct physical formulation of the problem and they do predict the observed current-voltage behavior in a qualitative way. For practical purposes, the graphical construction in Fig. 5 suggests an even simpler lumped-parameter model might be useful. Figure 6 indicates that within a range of current density the polarization due to internal ionic resistance is linearly related to current density. The deviation from purely ohmic behavior occurs at current densities which are significantly higher than are used in present fuel cells, and perhaps higher than one

might expect to use in practice due to the limitation of total cell resistance. This suggests that for practical purposes the resistance polarization can be calculated using Ohm's law with an effective internal resistance that can be calculated directly from the bulk resistivity of the electrolyte. By anology with diffusion transport in porous solids, we can relate the effective resistivity of the electrolyte in the catalyst layer to bulk resistivity by,

$$R_{eff} = \frac{R_{\Omega}\tau}{\Theta}$$

where τ is the tortuosity factor and Θ is the area for ionic flux per unit electrode area. We can measure Θ from the volume of electrolyte "taken up" by an electrode per unit porous volume, which has been found to be close to unity in electrodes of our type. Tortuosity factors for flow in a porous medium like carbon black (5-10 nm mean-pore size) are well-known and are typically 4-6, the larger value applying to larger molecules. The expected relation for the effective resistivity is therefore,

$$R_{eff} = 6\ R_{\Omega}.$$

According to the slope of the plot Fig. 7, the effective resistivity of the electrolyte in the catalyst layer was 12Ω-cm when the bulk resistivity was 1.6 Ω-cm, or 7.5 times the bulk resistivity, reasonable agreement with the expected relation. For practical purposes, it seems reasonable to apply the simple relation in equation (3) and to calculate the potential drop

within the electrode structure assuming purely ohmic resistance polarization for current densities below 500 mA/cm^2.

Phosphoric acid is not the only fuel cell electrolyte in which resistance polarization (and therefore anomalous current ratios) as been observed in air cathodes of the type used here. Table 1 gives a summary of results in other electrolytes with the graphitized carbon supported Pt electrocatalyst. Resistance polarization was lower in alkaline KOH cells than in H_3PO_4 due to the higher conductivity, and was significantly higher in CF_3SO_3H cells due to the higher resistivity of that electrolyte. In this table, the expected values are those computed from equation (3), and the observed values are those derived from the graphical construction method shown in Fig. 5. The agreement was good for current densities less than 500 mA/cm^2. In the current density range of 200-500 mA/cm^2, the O_2/air current ratios were 2.5-3.0, as expected from the mathematical model for resistance polarization.

There is another important practical consequence of resistance polarization that needs to be emphasized. Since resistance polarization is linearly dependent on catalytic layer thickness, this type of voltage loss will limit the loading of catalyst even when gas can be effectively supplied throughout the catalyst layer. As an example, consider, qualitatively, the case of a non-Pt catalyst that has a lower intrinsic activity (per unit weight of catalyst) than 10 w/o Pt on carbon. More catalyst must be used, resulting in more resistance polarization at high current density with this less active catalyst. For quantitaive purposes, assume a non-Pt catalyst has one-fifth of the activity of supported Pt with about the same pore

Table 1. Resistance Polarization in Fuel Cell Cathodes.[a]

Electrolyte	Bulk Resistivity (Ω-cm)	$\Delta\Phi_R$ Expected[b,c]	$\Delta\Phi_R$ Observed[c]
98 w/o H_3PO_4	1.6 (180°C)	30	40
70 w/o CF_3SO_3H	4.0 (70°C)	77	70
23 w/o NaOH	1.9 (70°C)	35	30
35 w/o KOH	0.9 (70°C)	18	15

[a] 5 mg/cm^2 of 5 w/o Pt on graphitized Vulcan XC-72R with 25-50 w/o TFE30B.

[b] expected value calculated from eq. (3) and bulk resistivity of acid.

[c] polarization in mV at a current density of 400 mA/cm^2.

distribution (tortuosity factor), as might be expected for an organometallic catalyst immobilized on a carbon black support. At low current density (<50 mA/cm^2), a 25 mg/cm^2 cathode of the non-Pt catalyst would have the same performance as a 5 mg/cm^2 cathode of supported Pt, but at high current density (>200 mA/cm^2) the higher resistance polarization in the non-Pt catalyst electrode drastically reduces the cathode potential, even with pure oxygen, relative to that of the Pt cathode. If one tries to compensate for this effect by using more than the activity ratio of catalyst, it is easily seen that in the more resistive electrolytes one has a no-win situation at high current density, i.e. it is impossible to achieve equivalent performance at high current density with catalysts significantly less active than supported Pt.

Izckowski and Cutlip[16] included the possible effects of finite electronic resistance in the catalyst layer, particularly interparticle contact resistance, on the total polarization. The effect of electronic resistance was not included in the analysis presented here, even though it is probably an important factor in the polarization behavior of real cells. For our purposes here, however, the omission is justified on both an experimental and theoretical basis. Experimentally, one can measure the purely electronic component of a "dry" electrode using standard techniques, and the possible contribution of electronic resistance can be calculated from the measured resistivity. It was found in this study that the average (spatially average) resistance is very low, and the contribution to total polarization is negligible at current densities below 500 mA/cm^2. Fundamentally, electronic resistance cannot contribute to the IR- corrected

polarization of electrodes in half-cells, since the electronic resistance is included in the IR as measured by the current-interruption technique,[13] i.e. the fast ($<10^{-6}$ sec) part of the potential decay corresponds to the ohmic potential drop between the current collector (at $x-\delta$ in Fig. 8) and the Luggin capillary (exterior to $x=0$).

ACKNOWLEDGMENTS

The author acknowledges valuable discussions with his former colleague Dr. W. Vogel of United Technologies Corporation who brought the current-ratio anomaly to my attention many years ago and who suggested that the prior analysis by Vdovichenko was pertinent. This work was performed under funding by the Electric Power Research Institute under Contract RP1200-5 under an agreement with the US Department of Energy under Contract No. DE-AC03-76SF00098.

APPENDIX

The mathematical analysis we give here follows the perturbation theory method used by Vdovichenko[20] for a physical model of hydrophobic gas-diffusion electrodes essentially identical to Fig. 8. The equations derived here, however, differ from those derived by Vdovichenko because a different kinetic expression is used. We use here the empirical form of rate equation derived from rotating disc electrode studies. The local current density (i) at any point (x,r) is given by

$$i = k\ c\ \exp\ (-2.3V^{*}/b)$$

where $V^{*} = V + \Delta\phi_e - \Delta\phi_M$. k is the empirical rate constant, c the local concentration of dissolved oxygen, and b is the empirical Tafel slope. V is the observed electrode potential relative to an arbitrary reference electrode, which corresponds to the potential difference between the current collector and ions in solution at the tip of the reference capillary; V^{*} is the potential at any point (x,r) in the catalyst relative to the reference electrode; $\Delta\phi_e$ is the potential drop (seen by ions in the electrolyte) between the pore mouth (x=o) and any point (x,r); and $\Delta\phi_M$ is the resistive potential drop in the catalyst phase between the current collector and the point (x,r). The reference capillary is assumed to be sufficiently close to the physical exterior of the electrode that we can neglect the potential difference between the tip and the pore mouth. Some further assumptions are made: i.) we assume $\Delta\phi_M = 0$ for the current densities and carbon materials used here; ii.) we assume that R, the radius of spherical agglomerates, is much smaller than δ, the thickness of the electrode; iii.) we shall neglect gas phase diffusion

so that the concentration of dissolved oxygen is not a function of x; iv.) we assume that the dissolved oxygen concentration difference through the liquid film covering the agglomerates is negligible. Independent tests have shown that for the current densities of interest here, which are well below the observed limiting currents for electrodes of this type, these assumptions are reasonable. The assumption that $R<<\delta$ means there is no variation in ϕ_e within a single agglomerate, so that the molecular diffusion problem may be solved independently of the ionic diffusion problem. The molecular diffusion problem for the spherical agglomerate is

$$n F \bar{D}_m \left(\frac{d^2 c}{dr^2} + \frac{2}{r} \frac{dc}{dr} \right) = \gamma i \tag{4}$$

or

$$\frac{d^2 c}{dr^2} + \frac{2}{r} \frac{dc}{dr} = \alpha^2 c \tag{5}$$

$$\alpha^2 = \left(\frac{\gamma k}{n F \bar{D}_m} \right) \exp. \left(-2.3 V^* / b \right)$$

where $\bar{D}_m$ is the effective diffusivity of oxygen in the porous agglomerate γ is the active (Pt) area per unit volume of agglomerate and n is the number of electrons per mole of oxygen consumed. The boundary conditions are

$$r = R \, , \, c = C_o \tag{6}$$

$$r = 0 \, , \, \frac{dc}{dr} = 0 \tag{7}$$

The solution of (5)-(7) is

$$C = C_o \left(\frac{R}{r}\right)\left(\frac{\sinh \alpha r}{\sinh \alpha R}\right)$$

Therefore the current from an agglomerate is

$$i = 4\pi R^2 nF\bar{D}_m \left(\frac{dc}{dR}\right)_R = 4\pi R\, nF\bar{D}_m C_o [\alpha R \coth \alpha R - 1]. \qquad (8)$$

For a binary electrolyte

$$\Delta\phi_e = - \frac{RT}{zF} \ln \bar{C}_e \qquad (9)$$

where z is the ionic valence, and $\bar{C}_e = C_e(x)/C_e(0)$ C_e being the ionic concentration at any point x in the liquid pore. Combining (3), (8) and (9) gives

$$i = G \left[\frac{R}{Lg}\ \bar{C}_e^{\,m/2} \coth \frac{R}{Lg}\ \bar{C}_e^{\,m/2} - 1\right] \qquad (10)$$

where $G = 4\pi R\, nF\, D_m\, C_o$, $\qquad Lg = \left[\frac{\gamma k}{nF\bar{D}_m} \exp(-2.3V/b)\right]^{-1/2}$

and $m = 2.3\ RT/zF$. The electrode current density, I, is related to the local current i by

$$\frac{dI}{dx} = - 4\pi R^2 N i \qquad (11)$$

where N is the number of agglomerates per unit volume. I has to equal the flux of $(HS)^+$ ions, which is given by a Fick's law representation

$$I = -\left(1 + \frac{1}{z}\right) F \bar{D}_e C_e^{\circ} \frac{d\bar{C}_e}{dx} \qquad (12)$$

where $\overline{D}_e$ is the effective diffusivity of $(HS)^+$ ions in the electrolyte, and will be affected by changes in electrode structure through the porosity of the agglomerates and the tortuosity of the liquid pore. Combining (10)-(12) results in the diffusion equation for $(HS)^+$ ions

$$\frac{d^2 \overline{C}_e}{dx^2} = \beta^2 \left(\frac{Lg}{R}\right)^2 \left[\left(\frac{R}{Lg}\right) \overline{C}_e^{\,m/2} \coth \left(\frac{R}{Lg}\right) \overline{C}_e^{\,m/2} - 1\right]$$

$$\beta^2 = \left[\frac{4\pi R^4 N G}{(1+\frac{1}{z}) F \overline{D}_e C_e^{\circ} Lg^2}\right] \tag{13}$$

with boundary conditions

$$\overline{C}_e = 1 , \quad x=0$$

$$\frac{d\overline{C}_e}{dx} = 0 , \quad x=\delta$$

Following Vdovichenko, we shall obtain an analytical solution for the two limiting cases $R \ll Lg$, $R \gg Lg$ by perturbation theory.

Case 1: $R \ll Lg$

Equation (13) reduces to

$$\frac{d^2\overline{C}_e}{dx^2} = \beta^2 \overline{C}_e^{\,m} \tag{14}$$

A small perturbation in $\overline{C}_e$ down the liquid pore can be written as

$$\overline{C}_e = 1 - \rho , \quad \rho \ll 1 \tag{15}$$

which results in the new expression

$$\frac{d^2\rho}{dx^2} = \beta^2 (m\rho - 1) \qquad (16)$$

$$\rho = 0 \quad , \quad x=0$$

$$\frac{d\rho}{dx} = 0 \quad , \quad x=\delta$$

The solution of (16) gives for the electrode current density

$$I = (1 + \frac{1}{z}) F \bar{D}_e C_e^\circ \frac{d\bar{C}_e}{dx}$$

$$I = (1 + \frac{1}{z}) F \bar{D}_e C_e^\circ m^{-1/2} \beta \tanh m^{1/2} \beta\delta \qquad (17)$$

This equation is easier to interpret physically when $\beta\delta$ takes on the extreme values,

$$I = \begin{cases} K_1 \delta R \gamma k C_o \exp(-2.3V/b) & \beta\delta << 1 \qquad (18) \\ (K_2 R \gamma k C_o)^{1/2} \exp(-2.3V/2b) & \beta\delta >> 1 \qquad (19) \end{cases}$$

In any given electrode structure where the assumption R << Lg applies, the polarization curve will exhibit the two regions of behavior characterized by equations (18) and (19) in some potential region, with a transition from (18) to (19) at overpotentials beyond some critical value. The constant K_1 is just a geometric factor

$$K_1 = 2\pi\ NR^2$$

and K_2 contains the electrolyte constants

$$K_2 = (K_1/m)(1 + \frac{1}{z})\ F\ \overline{D}_e\ C_e^{\circ}$$

Case 2: $R >> Lg$

Equation (13) reduces to

$$\frac{d^2\overline{C}_e}{dx^2} = \beta^2\ (\frac{Lg}{R})\ \overline{C}_e^{\,m/2} \tag{20}$$

The perturbation theory solution to this nonlinear problem follows closely that for (14) and gives

$$I = (1 + \frac{1}{z})F\ \overline{D}_e\ C_e^{\circ}\ (Lg/R)(2m)^{-1/2}\ \beta\ \tanh\ (m/2)^{1/2}\ (Lg/R)\beta\delta \tag{21}$$

Again the extremes of the tanh function give more useful forms,

$$I = \begin{cases} 2\ K_1\ \delta\ (nF\ \overline{D}_m\ \gamma\ k)^{1/2}\ C_o\ \exp(-2.3V/2b) & \beta\delta<<1 \quad (22) \\ \\ 2\ K_1^{1/2}\ (nF\overline{D}_m\ \gamma\ k)^{1/4}\ C_o^{1/2}\ \exp(-2.3V/4b) & \beta\delta>>1 \quad (23) \end{cases}$$

REFERENCES

1. C.A. Reiser, United States Patent 3,964,930, United Technologies assignee, 1976.
2. D.P. Bloomfield, United States Patent 4,004,947, United Technologies assignee, 1977 and references therein to earlier patents.
3. L.M. Handley, "Description of a Generic 11-MW Fuel Cell Power Plant for Utility Applications," Electric Power Research Institute Report EM-3161, 1983.
4. A.J. Appleby, J. Electrochem. Soc., 117 (1970) 641.
5. P. Stonehart and P. Ross, Electrochim. Acta 21 (1976) 441.
6. A. Wheeler, Adv. Catalysis 3 (1951) 249.
7. J. Giner and C. Hunter, J. Electrochem. Soc., 116 (1969) 1124.
8. H. Petrow and R Allen, United States Patent 2,512, Prototech Company assignee, 1976.
9. J. Bett, K. Kinoshita, K. Routsis and P. Stonehart, J. Catal. 29 (1973) 160.

10. P. Ross, "Oxygen Reduction on Supported Pt Alloys and Inter- metallic Compounds in Phosphoric Acid," Electric Power Research Institute Report EM-1553, 1980.

11. D. Ferrier, K. Kinoshita, J. McHardy, and P. Stonehart, J. Electroanal. Chem., 61 (1975) 233.

12. D. MacDonald and J. Boyack, J. of Chem. Engr. Data, 14 (1969) 380.

13. A. Falk and E. Lange, Z. Elektrochem. 54 (1950) 132.

14. H. Urbach, in "Fuel Cells Vol. 2," G. Young ed., Reinhold Publishing, New York and London, pp. 77-94.

15. I. Iliev, J. Mrha, A. Kaisheva and S. Gamburzev, J. Power Sources, 1 (1976/77) 35.

16. Iczkowski and M. Cutlip. J. Electrochem. Soc., 127 (1980) 1433.

17. P. Ross, J. Electrochem. Soc., 127 (1980) 2655.

18. K. Vetter, "Electrochemical Kinetics," Academie Press, New York and London, 1967, pp. 385-95.

19. A. Damjanovic and V. Brusie, Electrochim. Acta, 12 (1967) 615.

20. N. Vdovichenko, Elektrokhim. 8 (1972) 702.

FIGURE CAPTIONS

Fig. 1. Assembly diagram of the free-electrolyte fuel cell for air cathode polarization measurement: 1 - gas-diffusion electrodes; 2 - thin-film TFE gasket; 3 - Pt foil current collector; 4 - electrolyte fill hole; 5 - reference capillary.

Fig. 2. Polarization curves for gas-diffusion electrodes fabricated from platinized graphite black fed with 4% oxygen, 20% oxygen, and pure oxygen (balance nitrogen in mixtures). Current ratios at different potentials are noted on figure.

Fig. 3. Current ratios from electrode in Fig. 1 as a function of the current density.

Fig. 4. Polarization curves for gas-diffusion electrodes fabricated from platinized carbon black (10 wt% Pt-V, 0.25 mg Pt/cm^2) fed with 20% oxygen and air.

Fig. 5. Same electrode as in Fig. 1 with a dotted line showing the 5 x 20% oxygen curve as a function of potential. The difference in potential at constant current density between the observed pure oxygen curve and the projected 5 x 20% oxygen curve is denoted $\Delta\Phi_R$.

Fig. 6. Plots of resistance polarization, $\Delta\Phi_R$, versus current density as a function of catalyst layer thickness: □ - 0.004 cm; 0 - 0.008 cm; Δ - 0.016 cm. Catalyst was 5% Pt-GV.

Fig. 7. Polarization curves for a commercial PAFC cathode (10 wt% Pt-V, 0.5 mg Pt/cm^2) gas fed with oxygen and air.

Fig. 8. Physical model of a single electrolyte (HS^+) filled pore formed by connected spherical aggregates of platinized carbon prime particles.

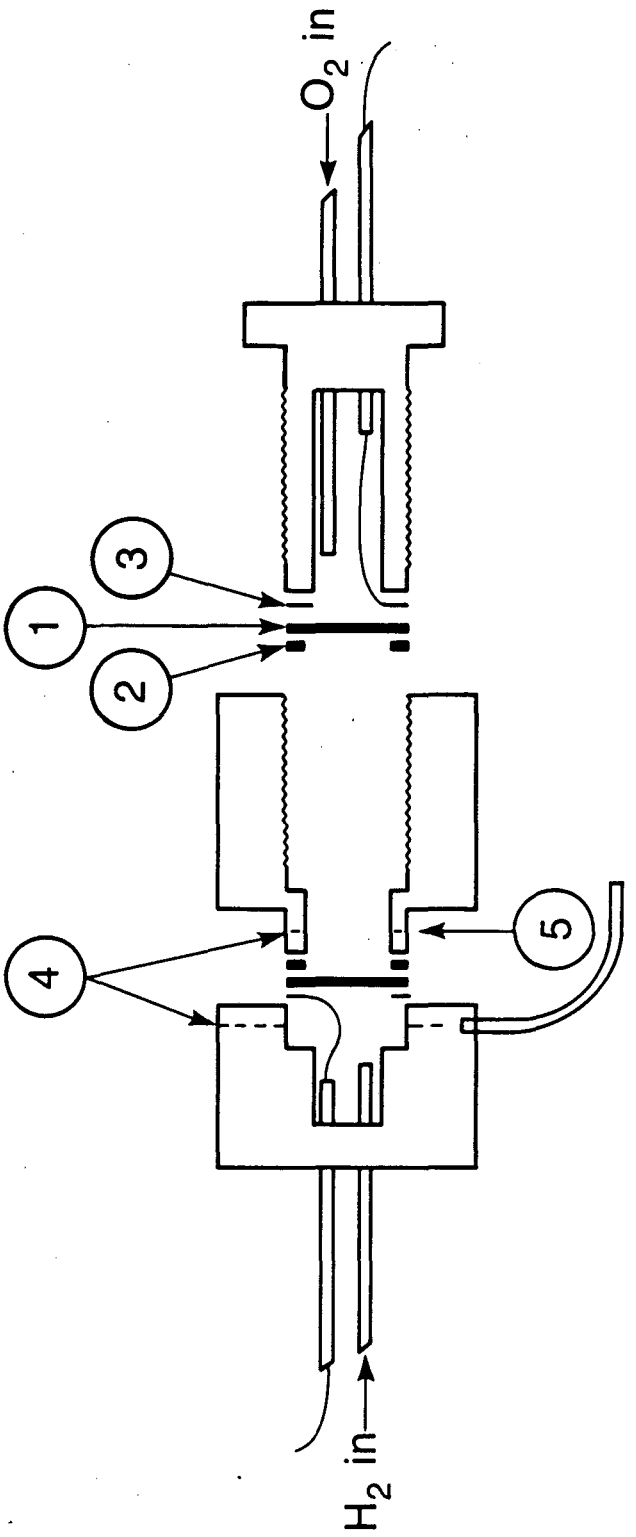

XBL 863-6193

Fig. 1

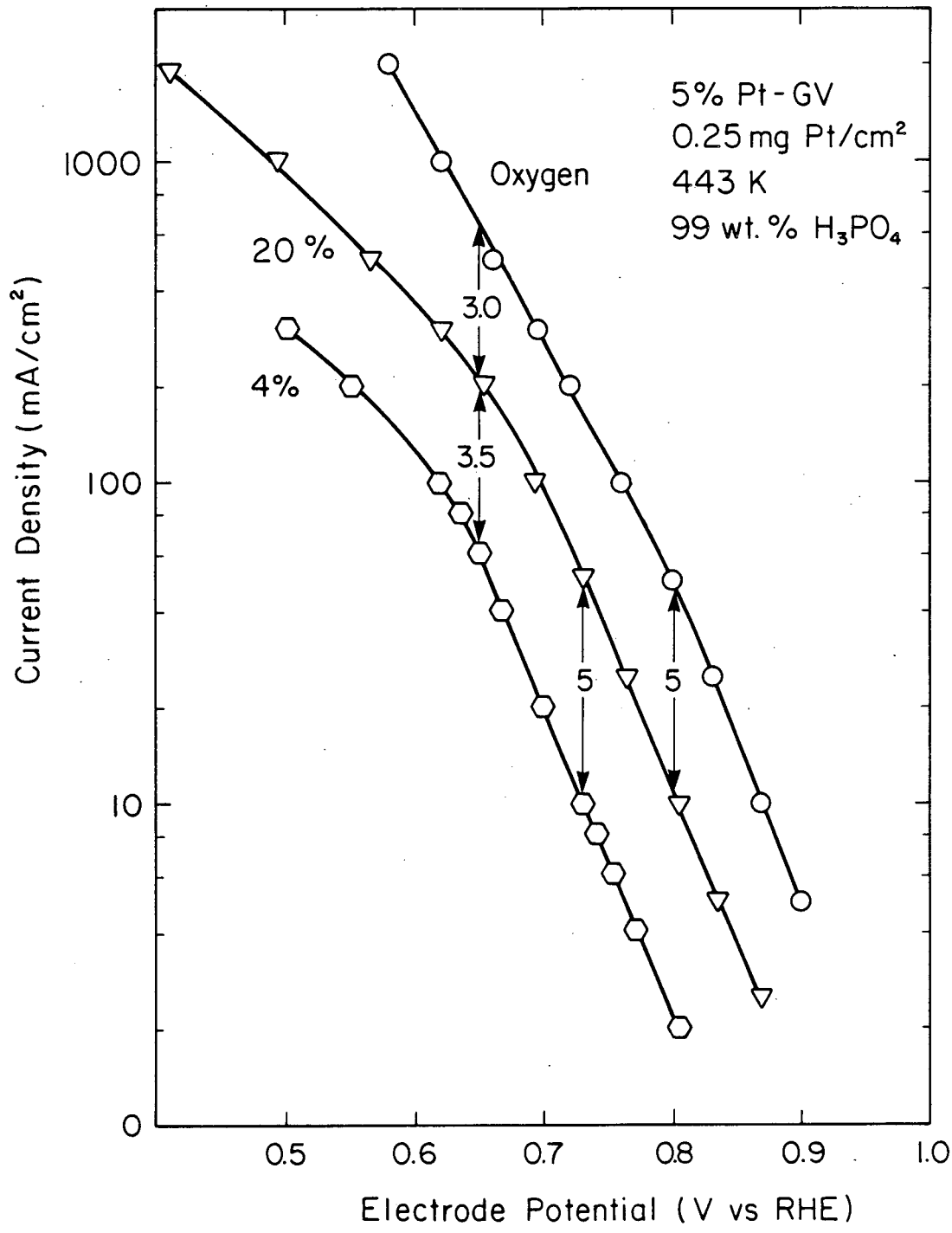

XBL 8512-12679

Fig. 2

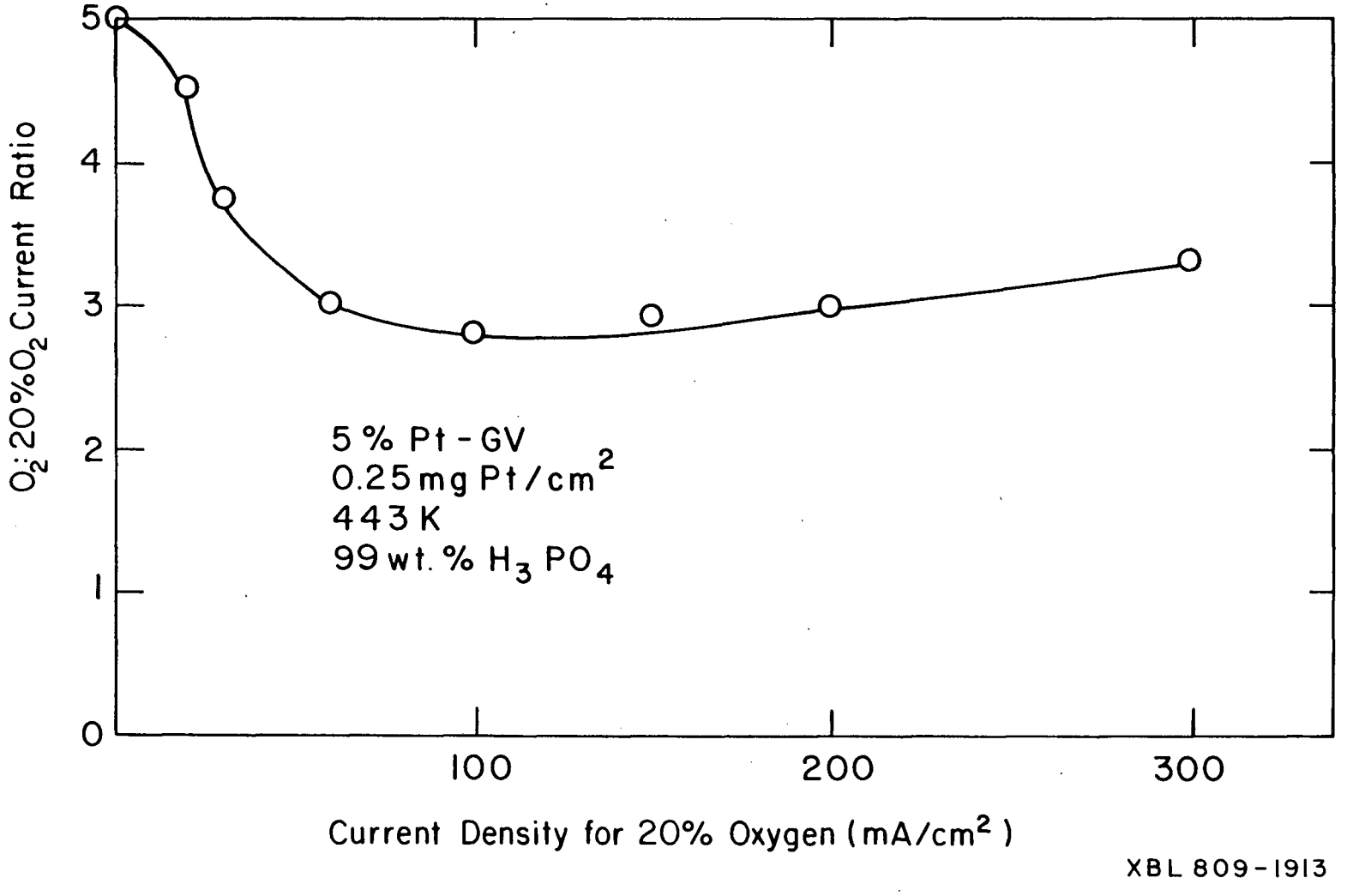
5
4
3
2
1
0
100
200
300
O_2:20%O_2 Current Ratio
Current Density for 20% Oxygen (mA/cm^2)
5 % Pt - GV
0.25 mg Pt/cm^2
443 K
99 wt. % H_3PO_4
XBL 809-1913

Fig. 3

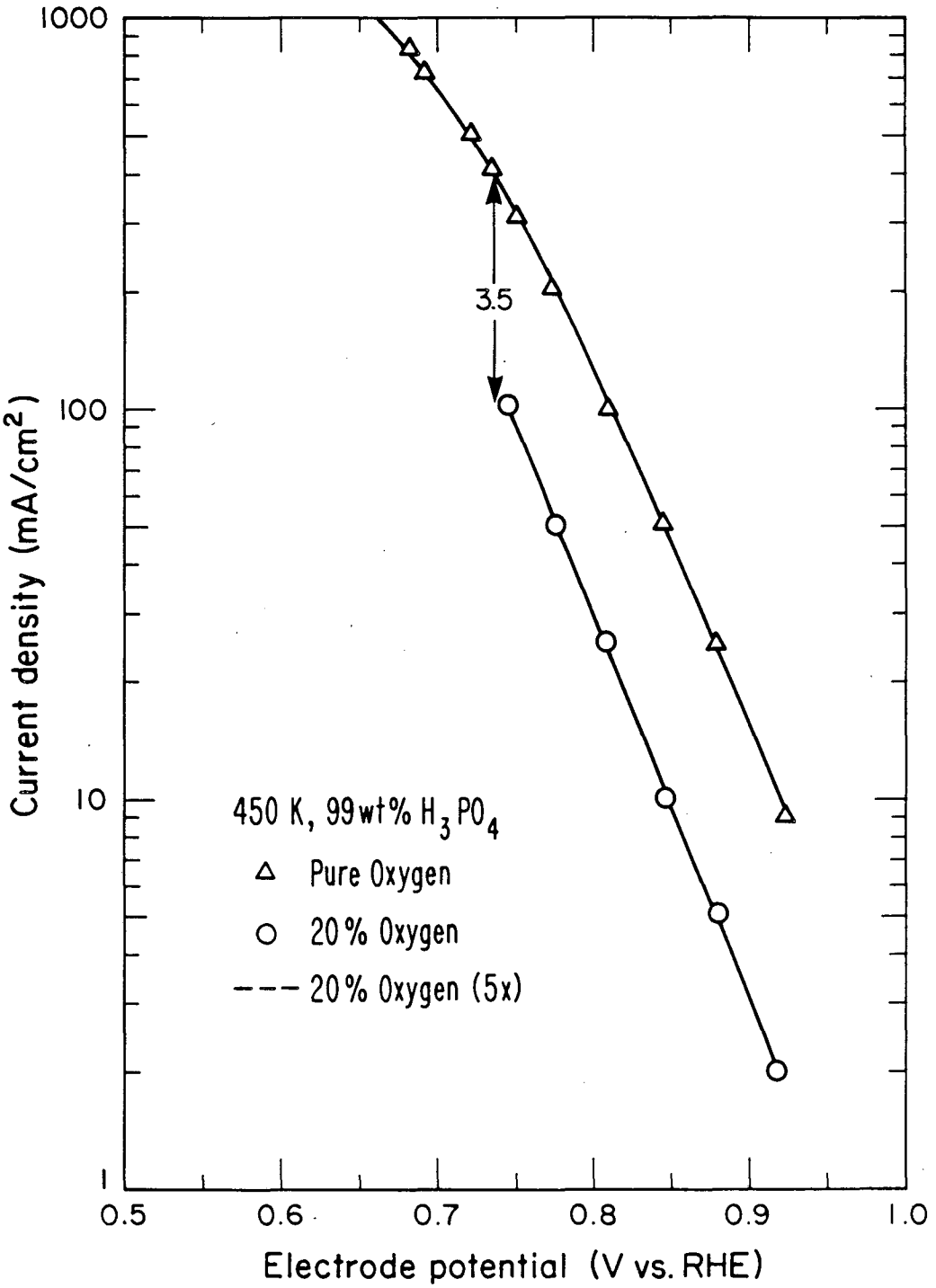

XBL 794-1113

Fig. 4

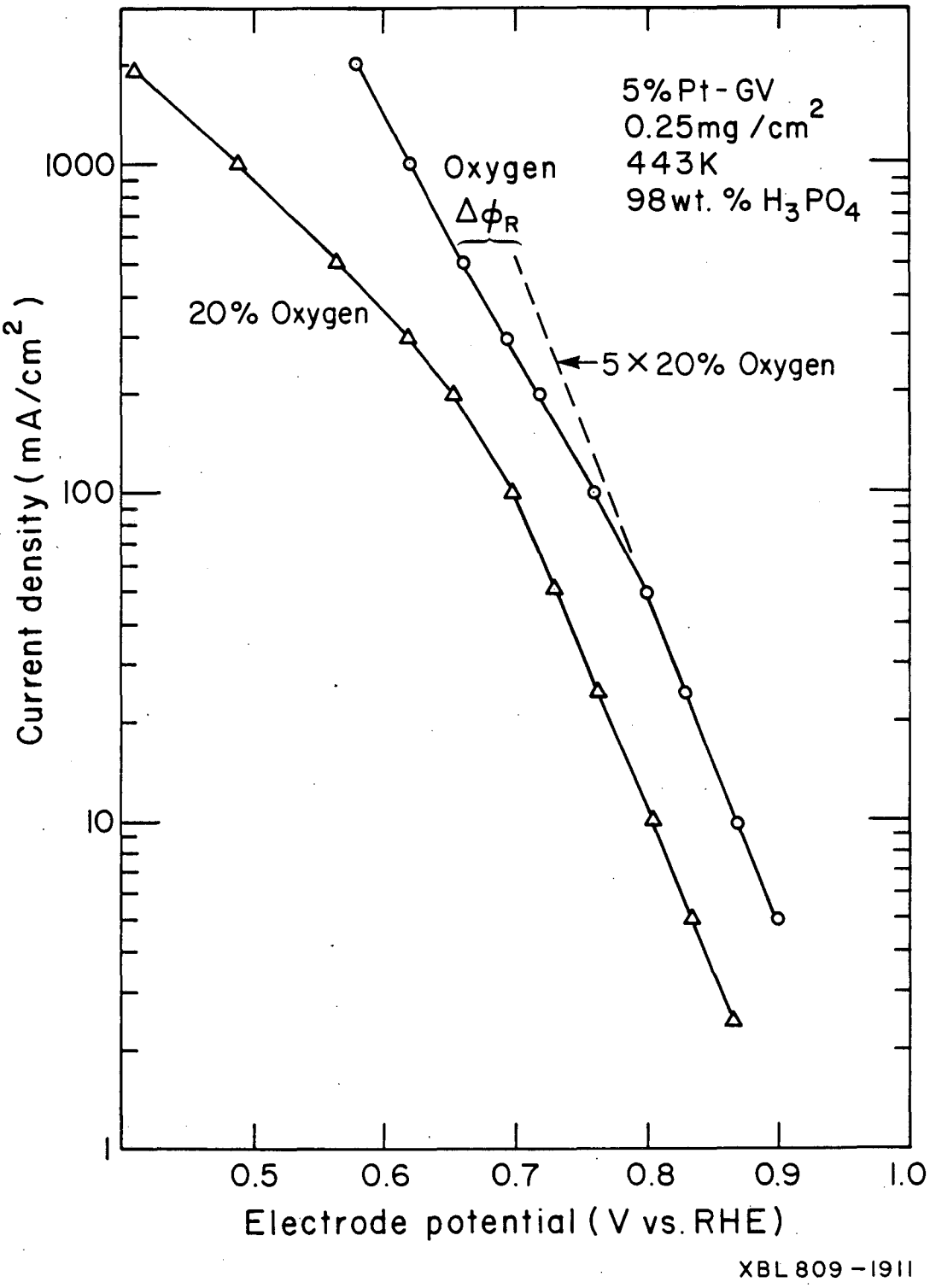
5% Pt - GV
0.25mg /cm²
443K
98wt. % H₃PO₄
Oxygen
Δφ_R
20% Oxygen
5 × 20% Oxygen
Current density (mA/cm²)
1000
100
10
1
0.5
0.6
0.7
0.8
0.9
1.0
Electrode potential (V vs. RHE)
XBL 809 - 1911

Fig. 5

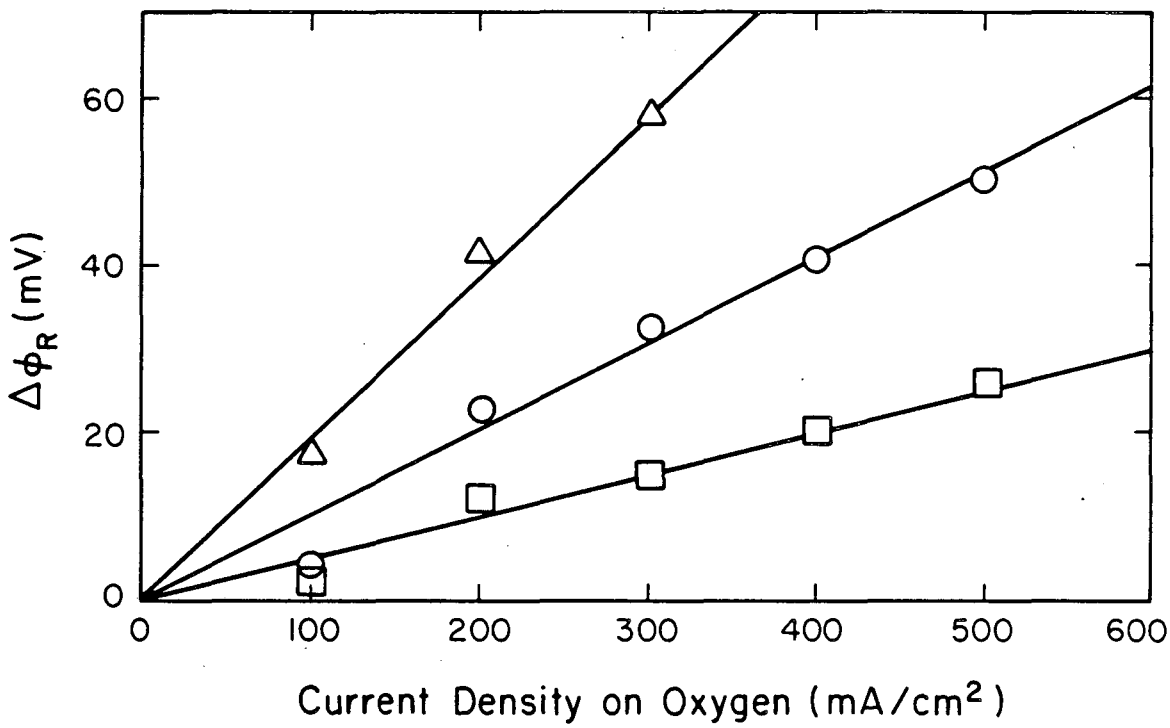

XBL 8512-12436

Fig. 6

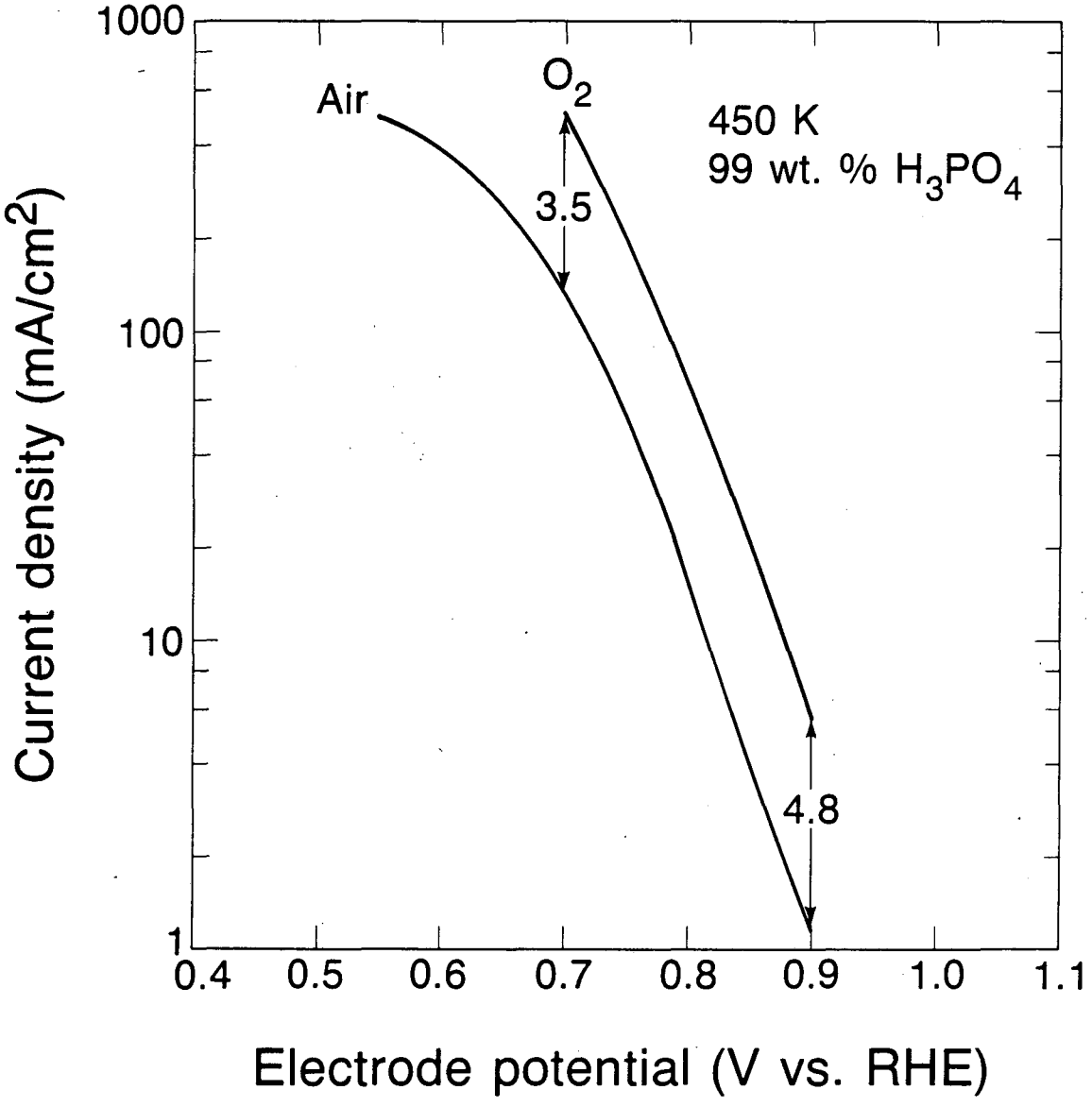

XBL 863-6191

Fig. 7

PHYSICAL MODEL OF SINGLE PORE

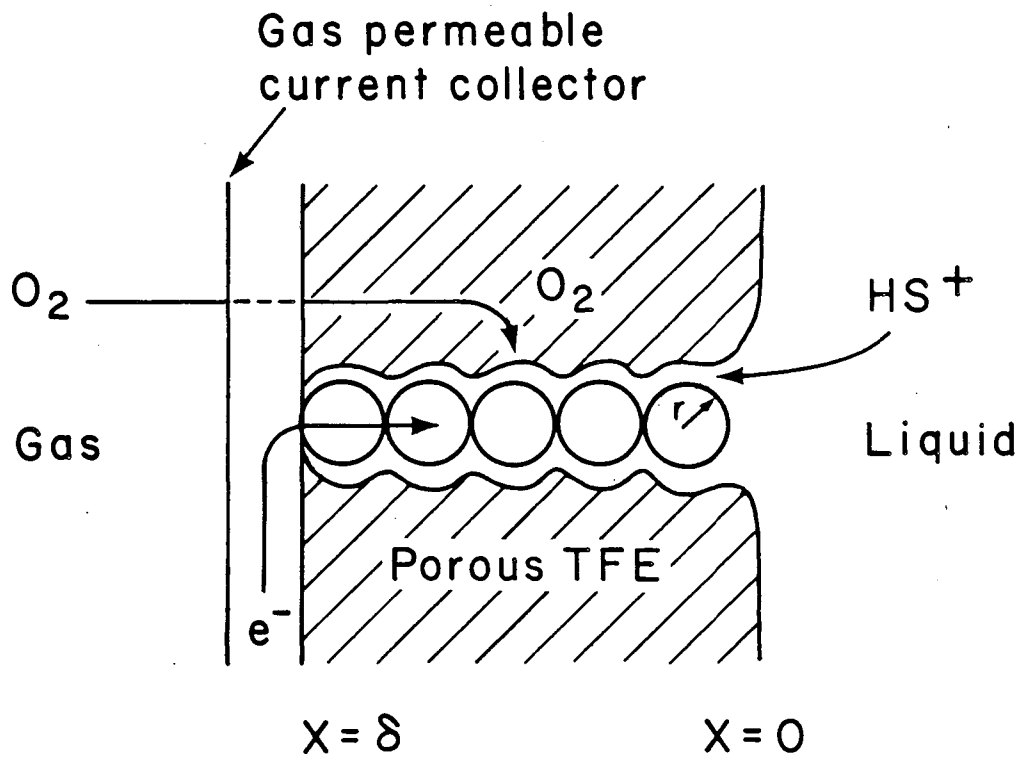

XBL 809-1912

Fig. 8

LAWRENCE BERKELEY LABORATORY
TECHNICAL INFORMATION DEPARTMENT
UNIVERSITY OF CALIFORNIA
BERKELEY, CALIFORNIA 94720